Volume 13
Number 2
14 January 2021
Pages 149–280

Analytical Methods

rsc.li/methods

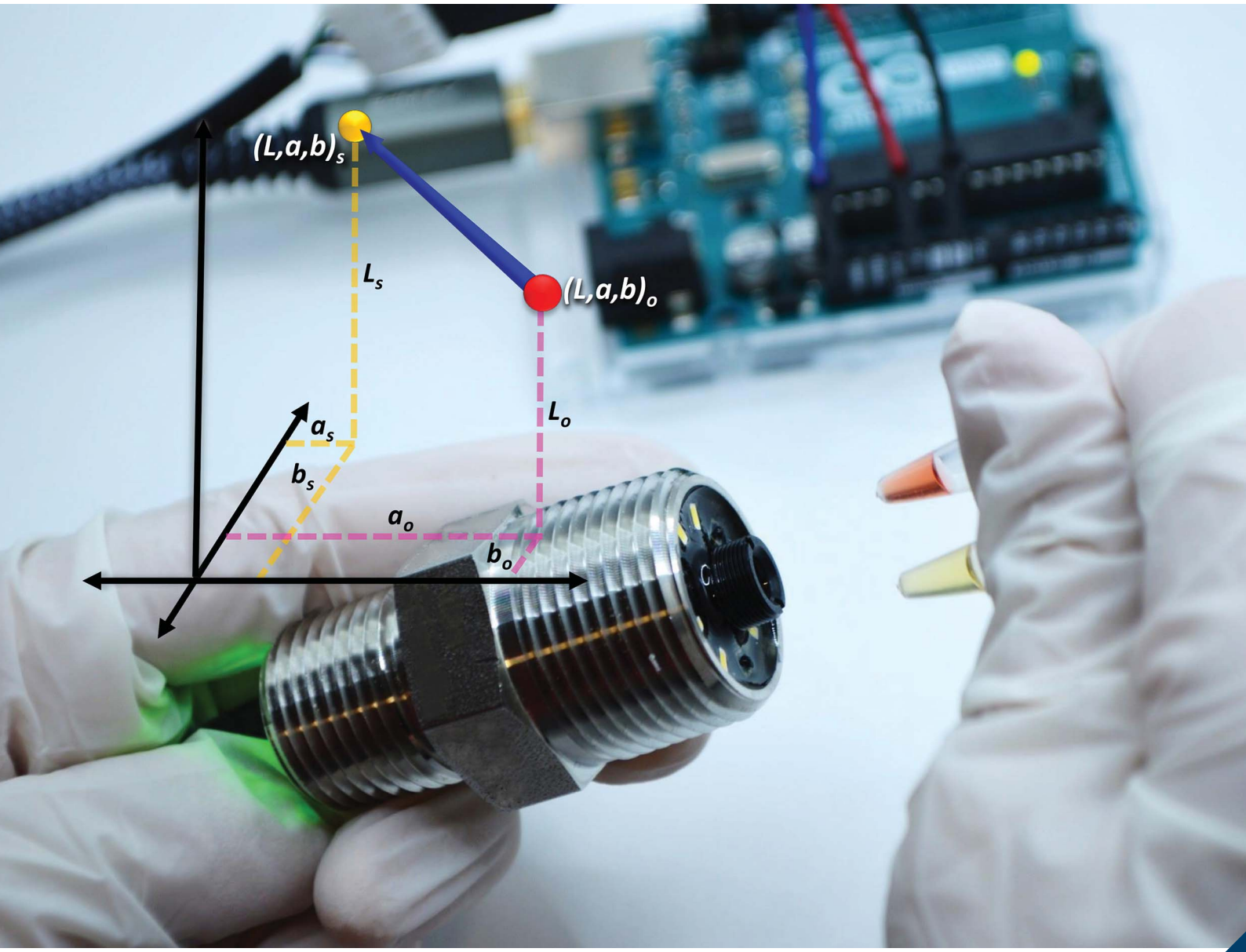

ISSN 1759-9679

COMMUNICATION

Grissel Trujillo-de Santiago, Mario Moisés Alvarez *et al.*
Colorimetric loop-mediated isothermal amplification (LAMP) for cost-effective and quantitative detection of SARS-CoV-2: the change in color in LAMP-based assays quantitatively correlates with viral copy number

ROYAL SOCIETY OF CHEMISTRY

Analytical Methods

ROYAL SOCIETY OF CHEMISTRY

COMMUNICATION

View Article Online
View Journal | View Issue

Cite this: *Anal. Methods*, 2021, **13**, 169

Colorimetric loop-mediated isothermal amplification (LAMP) for cost-effective and quantitative detection of SARS-CoV-2: the change in color in LAMP-based assays quantitatively correlates with viral copy number†

Received 1st September 2020
Accepted 30th November 2020

DOI: 10.1039/d0ay01658f

rsc.li/methods

Everardo González-González,*[ab] Itzel Montserrat Lara-Mayorga,[ac] Iram Pablo Rodríguez-Sánchez,[de] Yu Shrike Zhang,[f] Sergio O. Martínez-Chapa,[c] Grissel Trujillo-de Santiago*[ac] and Mario Moisés Alvarez*[ab]

We demonstrate a loop-mediated isothermal amplification (LAMP) method to detect and amplify SARS-CoV-2 genetic sequences using a set of in-house designed initiators that target regions encoding the N protein. We were able to detect and amplify SARS-CoV-2 nucleic acids in the range of 62 to 2 × 10^5 DNA copies by this straightforward method. Using synthetic SARS-CoV-2 samples and RNA extracts from patients, we demonstrate that colorimetric LAMP is a quantitative method comparable in diagnostic performance to RT-qPCR (*i.e.*, sensitivity of 92.85% and specificity of 81.25% in a set of 44 RNA extracts from patients analyzed in a hospital setting).

Introduction

By the end of December 2020, more than 80 million positive cases of COVID-19 were officially reported across the globe.[1] Even developed countries, such as the USA, England, France, and Germany, are still struggling to mitigate the propagation of SARS-CoV-2 by implementing social distancing and widespread testing. Less developed regions, such as Latin America, India, and Africa are now the epicenter of COVID-19; these territories are woefully lacking in the finances or the mounted infrastructure for diagnosis of this pandemic infection. Rapid and massive testing of thousands of possibly infected subjects has been an important component of the strategy of the countries that are effectively mitigating the spreading of COVID-19 among their populations (*i.e.*, China,[2] South Korea,[3] and Singapore[4]). By comparison, developing countries with high demographic densities, such as México,[5] India,[6] or Brazil[7] have not be able to implement a sufficient number of centralized laboratories for rapid large-scale testing for COVID-19.

Many methodologies have been proposed recently to deliver cost-effective diagnosis (*i.e.*, those based on immunoassays[8–11] or specific gene hybridization assisted by CRISPR-Cas systems[12,13]). While immunoassays are an accurate and efficacious tool for assessing the extent of the infection for epidemiological studies,[14] their usefulness is limited to the identification of infected subjects during early phases of infection,[11,15] a critical period for infectiveness. For instance, experimental evidence collected from a small number of COVID-19 patients (9 subjects) showed that 100% of them produced specific immunoglobulins G (IgGs) for SARS-CoV-2 within two weeks of infection, but only 50% of them did during the first week post infection.[16]

Nucleic acid amplification continues to be the gold standard for the detection of viral diseases in the early stages,[17–21] and very small viral loads present in symptomatic or asymptomatic patients can be reliably detected using amplification based methods, such as polymerase chain reaction (PCR),[22,23] recombinase polymerase amplification (RPA),[24] and loop-mediated isothermal amplification (LAMP).[25–27]

During the last two pandemic events with influenza A/H1N1/2009 and COVID-19, the Centers for Disease Control and Prevention (CDC) and the World Health Organization (WHO) recommended real-time quantitative PCR (RT-qPCR) methods as the gold standard for official detection of positive cases.[15,28] However, the reliance on RT-qPCR often leads to dependence on centralized laboratory facilities for testing.[15,28–31] To resolve this drawback, isothermal amplification reaction schemes (*i.e.*, LAMP and RPA) have been proposed as alternatives to PCR-based methods and devices for point-of-care settings.[30,32,33]

[a]*Centro de Biotecnología-FEMSA, Tecnologico de Monterrey, CP 64849, Monterrey, NL, Mexico. E-mail: Mario.alvarez@tec.mx; Grissel@tec.mx*

[b]*Departamento de Bioingeniería, Tecnologico de Monterrey, CP 64849, Monterrey, NL, Mexico*

[c]*Departamento de Ingeniería Mecátrónica y Eléctrica, Tecnologico de Monterrey, CP 64849, Monterrey, NL, Mexico*

[d]*Universidad Autónoma de Nuevo León, Facultad de Ciencias Biológicas, Laboratorio de Fisiología Molecular y Estructural, 66455, San Nicolás de los Garza, NL, Mexico*

[e]*Alfa Medical Center, Guadalupe, CP 67100, NL, Mexico*

[f]*Division of Engineering in Medicine, Department of Medicine, Brigham and Women's Hospital, Harvard Medical School, Cambridge 02139, MA, USA*

† Electronic supplementary information (ESI) available. See DOI: 10.1039/d0ay01658f

The urgency of using reliable molecular-based point of care (POC) methods for massive diagnostic during epidemiological emergencies has become even more evident during the current COVID-19 pandemics.[28,34,35]

In these times of COVID-19,[36] scientists and philanthropists around the globe have worked expeditiously on the development of rapid and portable diagnostics for SARS-CoV-2. Several reports have demonstrated the use of colorimetric LAMP-based methods for diagnosis of pandemic COVID-19.[37–42] Some of these reports use phenol red, a well-known pH indicator, to assist in the visual discrimination between positive and negative samples.[37,42,43]

In this study, we demonstrate the use of a simple embodiment of a colorimetric LAMP protocol for the detection and amplification of synthetic samples and actual RNA samples from patients of SARS-CoV-2, the causal viral agent of COVID-D. In this LAMP-based strategy, the discrimination between positive and negative samples is achieved by visual inspection. We quantitatively analyze differences in color between positive (yellow) and negative samples (red) using color decomposition and analysis in the color CIELab space.[44] Moreover, we compare the sensibility of this LAMP colorimetric method *versus* PCR protocols. This simple strategy is potentially adequate for the fast deployment of diagnostic efforts in the context of COVID-19 pandemics.

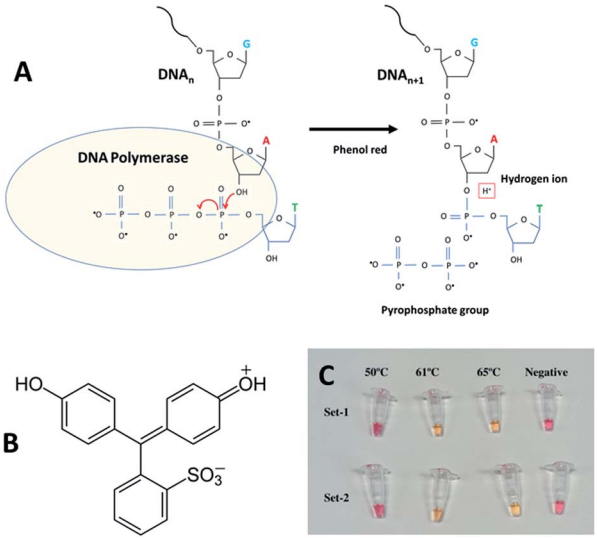

Fig. 1 Initiators and pH indicator for SARS-CoV-2 detection using a colorimetric LAMP method. (A) The LAMP reaction scheme. (B) Chemical structure of phenol red. (C) Two different sets of LAMP primers were used for successfully targeting a gene sequence encoding the SARS-CoV-2 N protein. Successful targeting and amplification are clearly evident to the naked eye: positive samples shift from red to yellow.

Rationale

Here we demonstrate a simple diagnostic method for the detection of SARS-CoV-2, the causal agent of COVID-19. The method is based on the amplification of the genetic material of SARS-CoV-2 using LAMP. The amplification is conducted using a commercial reaction mix in commercial and widely available 200 μL Eppendorf PCR tubes. LAMP is an isothermal process that can be conducted using commercially available thermoblocks, economical end-point thermo cyclers (*i.e.*, miniPCR[22,23] from Amplyus, USA), or other means to guaranty a constant temperature in the range of 60 to 65 °C. Moreover, we demonstrate that this colorimetric method is quantitative; the advance of the amplification reaction can be quantitatively followed by the progression in color, from red to yellow. In the following section, we briefly discuss the mechanisms of amplification and visual discrimination between positive and negative samples.

Results and Discussion

Colorimetric LAMP amplification

The presence of phenol red within the LAMP reaction mix allows for naked-eye discrimination between positive and negative samples (Fig. 1). The reaction mix is coupled with the pH color transition of phenol red, a widely used pH indicator, which shifts in color from red to yellow at pH 6.8. During LAMP amplification, the pH of the reaction mix continuously evolves from neutrality to acidic values as protons are produced.[25,45] The mechanism of production of hydrogen ions (H^+) during amplification in weakly buffered solutions has been described.[45] DNA polymerases incorporate a deoxynucleoside triphosphate into the nascent DNA chain. During this chemical event, a pyrophosphate moiety and a hydrogen ion are released as byproducts (Fig. 1A). This release of hydrogen ions is quantitative, according to the reaction scheme illustrated in Fig. 1. The caudal of H^+ is high, since it is quantitatively proportional to the number of newly integrated dNTPs. In fact, the quantitative production of H^+ is the basis of previously reported detection methods, such as the semiconductor sequencing technology operating in Ion Torrent sequencers.[46]

In the initially basic (pH ~ 7.5–8.5) and weakly buffered reaction mixes, the production of H^+ during LAMP amplification progressively and rapidly shifts the pH across the threshold of phenol red (Fig. 1B). Moreover, the pH shift is clearly evident to the naked eye, thereby freeing the user from reliance on spectrophotometric instruments and facilitating simple implementation during emergencies (Fig. 1C). Images in Fig. 2C show representative colors of the amplification reaction mixes contained in Eppendorf PCR tubes after incubation for 30 min. Three different incubation temperatures were tested (50, 60, and 65 °C) and two different sets of LAMP-primers (α and β) were used (Table 1).

Both sets of primers performed equivalently based on visual inspection in the three temperature conditions tested. Discrimination between positive and negative controls is possible using only the naked eye to discern the reaction products from amplifications conducted at 60 and 65 °C. No or negligible amplification was evident at 50 °C or in the control group. Furthermore, we were able to successfully discriminate between positive and negative samples using LAMP reaction mix already added with primers and kept at 20 °C or 4 °C for 24, 48, 72, and 96 h (Fig. S1†). The stability of the reaction, the

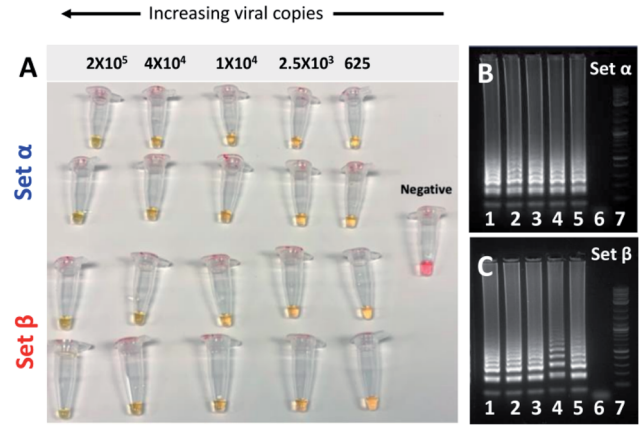

Fig. 2 Two different sets of LAMP-primers were used for successfully targeting of a gene sequence encoding the SARS-CoV-2 N protein. (A) LAMP primer sets α and β both enable the amplification of synthetic samples of SARS-CoV-2 nucleic acids in a wide range of template concentrations, from 625 to 2.0 × 10^5 DNA copies of SARS-CoV-2 when incubated for 50 minutes at a temperature range from 60 to 65 °C. (B and C) Agarose gel electrophoresis of DNA amplification products generated by targeting two different regions of the sequence coding for SARS-CoV-2 N protein. Two different primer sets were used: (B) primer set α, and (C) primer set β. The initial template amount was gradually decreased from left to right: 2.0 × 10^5 DNA copies (lane 1), 4.0 × 10^4 copies, (lane 2), 1.0 × 10^4 copies (lane 3), 2.5 × 10^3 copies (lane 4), 625 copies (lane 5), negative control (lane 6), and molecular weight ladder (lane 7). Panel (B) and (C) corresponds to portions of the full-length gels presented in ESI Fig. S2A and B,† respectively.

isothermal nature of the amplification process, and its independence from specialized equipment greatly simplifies the logistic of implementation of this diagnostic method outside centralized labs.

Analysis of sensitivity

We conducted a series of experiments to assess the sensitivity of the LAMP reactions in a miniPCR apparatus using the two sets of primers (α and β; Table 1). The amplification proceeds with sufficient quality to also allow proper visualization of the amplification products in electrophoresis gels, even at low nucleic acid concentrations. We observed that amplification proceeded successfully in a wide range of viral loads, from 625 to 5 × 10^5 copies in experiments using synthetic SARS-CoV-2 nucleic acid material (Fig. 2A). Incubation periods of up to 1 h at 68 °C did not induced false positives and were able to amplify as few as ~62 copies of SARS-CoV-2 synthetic genetic material (Fig. S1†). The actual viral load of COVID-19 in nasal swabs from patients has been estimated to fall within the range of 10^5 to 10^6 viral copies per mL.[47] Then, discrimination between positive and negative samples (controls) can be clearly established by the naked eye in all reactions incubated for 50 min, regardless of the number of viral copies present.

In addition, we did not observe any non-specific amplification in negative samples (*i.e.*, containing synthetic genetic material from EBOV, or only initiators) incubated for 50 min at 65 °C.

We corroborated the amplification by visualizing LAMP products with gel electrophoresis for the different viral loads tested. Fig. 2B and C show agarose gels of the amplification products of each one of the LAMP experiments, where two different sets of primers (α and β) were used to amplify the same range of concentrations of template (from 625 to 2 × 10^5 synthetic viral copies). We were able to generate a visible array of bands of amplification products, a typical signature of LAMP, for both LAMP primer sets and across the whole range of synthetic viral loads. Indeed, both primer sets rendered similar amplification profiles.

We showed that, after only 30 min of incubation at 65 °C, samples containing a viral load in the range of 10^4 to 10^5 copies could be clearly discriminated from negative samples by visual inspection with the naked eye (Fig. 3A). Samples with a lower viral load were clearly discriminated when the LAMP reaction was incubated for 50 min. These results are consistent with those of other reports in which colorimetric LAMP, assisted by phenol red, has been used to amplify SARS-CoV-2 genetic material.[37,48] We did not observed false positive cases in experiments where synthetic samples containing EBOV genetic material or only primers were incubated at 65 °C for 1 h.

Table 1 Primer sequences used in LAMP amplification experiments. Two different sets of primers were used, directed at the RNA sequence encoding the N sequence of the SARS-CoV-2

Set	Description	Primers sequence (5′ > 3′)
Primer set α	2019-nCoV 1-F3	*TGGACCCCAAAATCAGCG*
	2019-nCoV 1-B3	*GCCTTGTCCTCGAGGGAAT*
	2019-nCoV 1-FIP	*CCACTGCGTTCTCCATTCTGGTAAATGCACCCCGCATTACG*
	2019-nCoV 1-BIP	*CGCGATCAAAACAACGTCGGCCCTTGCCATGTTGAGTGAGA*
	2019-nCoV 1-LF	*TGAATCTGAGGGTCCACCAA*
	2019-nCoV 1-LB	*TTACCCAATAATACTGCGTCTTGGT*
Primer set β	2019-nCoV 2-F3	*CCAGAATGGAGAACGCAGTG*
	2019-nCoV 2-B3	*CCGTCACCACCACGAATT*
	2019-nCoV 2-FIP	*AGCGGTGAACCAAGACGCAGGGCGCGATCAAAACAACG*
	2019-nCoV 2-BIP	*AATTCCCTCGAGGACAAGGCGAGCTCTTCGGTAGTAGCCAA*
	2019-nCoV 2-LF	*TTATTGGGTAAACCTTGGGGC*
	2019-nCoV 2-LB	*TAACACCAATAGCAGTCCAGATGA*

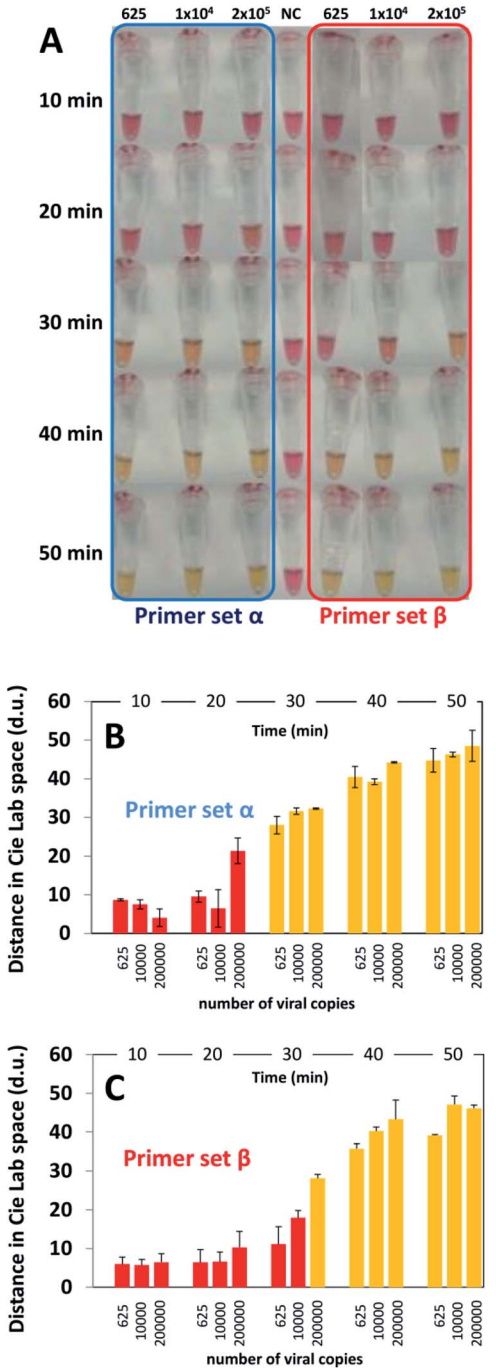

Fig. 3 Evaluation of the sensitivity of the combined use of a colorimetric LAMP method assisted by the use of phenol red. (A) Sensitivity trials using different concentrations of the template (positive control) and two different primers sets: α (indicated in blue) and β (indicated in red). Photographs of the Eppendorf PCR tubes containing positive samples and negative controls were acquired using a smartphone. (C and D) Distance in the color CIELab space between negative controls (red) and samples containing different concentrations of SARS-CoV-2 nucleic acid material (*i.e.*, 625, 10 000, and 200 000 synthetic copies) analyzed after different times of incubation (*i.e.*, 10, 20, 30, 40, and 50 minutes) at 65 °C. The analysis of color distances is presented for amplifications conducted using primer set (B) α and (C) β.

Feasibility of real-time quantification

Here, we further illustrate the deterministic and quantitative dependence between the concentration of the amplification product and the color signal produced during this colorimetric LAMP reaction. For this purpose, we simulated real-time amplification experiments by conducting a series of amplification reactions using initial amounts of 625, 1×10^4, and 2×10^5 copies of synthetic SARS-CoV-2 genetic material in a miniPCR apparatus. We extracted samples from a miniPCR thermal cycler operated isothermally after 0, 10, 20, 30, 40, and 50 min of incubation at 65 °C. The color of these samples was documented as images that were captured using a smart phone (iPhone 7) against a white background (Fig. 3A). The images were analyzed using the application Color Companion® for the iPhone or iPad. Briefly, color images were decomposed into their CIELab space components. In the CIELab color space, each color can be represented as a point in a 3D-space, defined by the values L, a, and b.[44] In this coordinate system, L is the luminosity (which ranges from 0 to +100), a is the blue-yellow axis (which ranges from −50 to 50), and b is the green-red axis (which ranges from −50 to 50) (Fig. S3†). The difference between two colors can be quantitatively represented as the distance (in distance units (d.u.)) between the two points that those colors represent in the CIELab coordinate system. For the colorimetric LAMP reaction mixture used in our experiments, the spectrum of possible colors evolves from red (for negative controls and negative samples) to yellow (for positive samples). Conveniently, the full range of colors for samples and controls can be represented in the red and yellow quadrant defined by L [0,100], a [0,50], and b [0,50]. For instance, the difference between the color of a sample (at any time of the reaction) and the color of the negative control (*e.g.*, red; $L = 53.72 \pm 0.581$, $a = 38.86 \pm 2.916$, and $b = 11.86 \pm 0.961$) can be calculated in the CIELab space. We determined the distance in the CIELab space between the color of samples taken at different incubation times that contained SARS-CoV-2 genetic material and negative controls. We repeated this calculation for each of the LAMP primer sets that we used, namely primer set α (Fig. 3B) and β (Fig. 3C). Our results suggest that the color difference between the samples and negative controls is quantifiable. Therefore, color analysis may be implemented to assist the discrimination between positives and negatives.

Furthermore, imaging and color analysis techniques may be implemented in this simple colorimetric LAMP diagnostic strategy to render a quantitative LAMP (qLAMP). In Fig. 4A we evaluate the distance in the CIELab color space of samples containing different quantities (625, 1×10^4, and 2.5×10^5 copies) of SARS-CoV-2 synthetic materials.

Interestingly, we observed significant differences in the performance of the two LAMP primer sets used in the experiments reported here (Fig. 3B and C and 4). Our results suggest that primer set α enabled faster amplification in samples with fewer viral copies. Consistently, this primer set yielded positive discrimination in 30 min for samples with 625 viral copies (Fig. 4A). The use of primer set β enabled similar differences in color, measured as distances in the CIELab 3D-space, but these

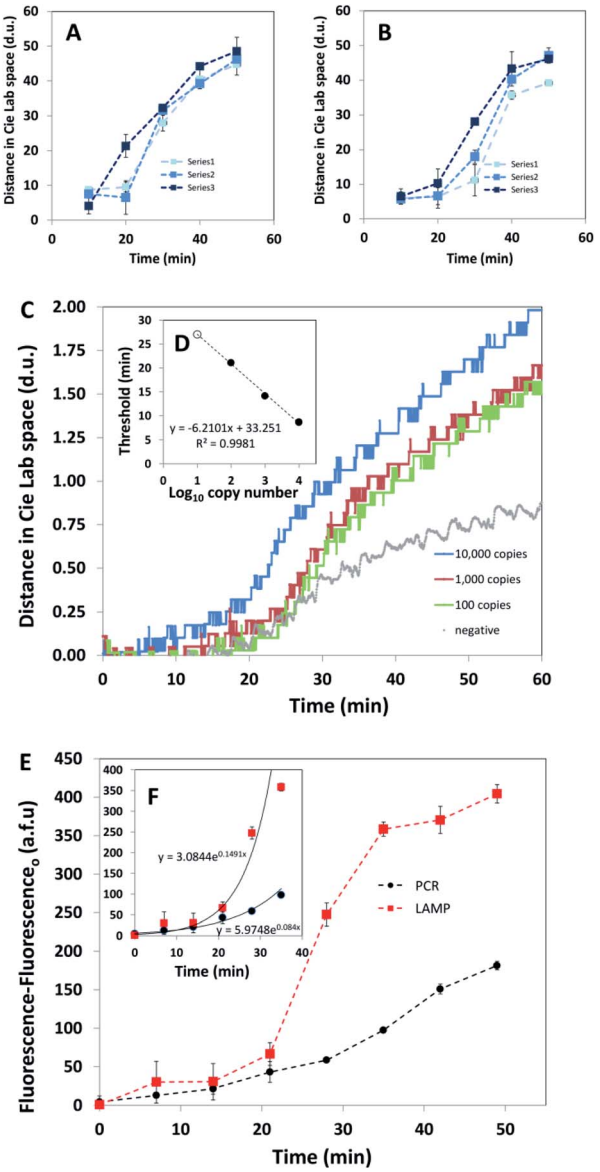

Fig. 4 Time progression of the distance in color with respect to negative controls (red color) in the CIELab space for positive SARS-CoV-2 samples containing 625 (light blue, ■), 1×10^4 (medium blue, ■), and 2.5×10^6 (dark blue, ■) copies of synthetic of SARS-CoV-2 nucleic acids. Results obtained in experiments using (A) primer set α, and (B) primer set β. (C) Progression of the color distance, with respect to the initial color of the sample, in samples containing 100 copies (green line), 1000 copies (red line), and 10 000 copies (blue line) of synthetic SARS-CoV-2 genetic material. The color progression for a negative sample is indicated with grey symbols. Only the β primer set was used in this experimental set. (D) Correlation between copy number and time threshold for positive diagnostic. (E) Comparison between the performance of PCR and LAMP in a simulated real-time experiment. Progression of the fluorescence signal, as measured with a plate reader, in PCR (black circles) and LAMP (red squares) experiments. The inset (F) shows a zoomed image at the exponential stage of the amplification process.

took longer times to emerge (*i.e.*, 40 min; Fig. 4B). The primers in set α may be targeting more stable regions or may show stronger binding affinity for the N-gene sequence in SARS-CoV-2 than primers in set β. These findings suggest that primer set α should be preferred for final-point implementations of this colorimetric LAMP method. However, primer set β may better serve the purpose of a real-time implementation. While primer set α produced similar trajectories of evolution of color in samples that contained 1.0×10^4 and 2.0×10^5 viral copies (Fig. 4A), primer set β was better at discriminating between amplifications produced from different initial viral loads (Fig. 4B).

Alternatively, the progression of color during the amplification reaction can be monitored in real time using commercially available color sensors. From these data, the change in the color distance in the CiELab space (or in any other color space) can be continuously calculated to render a quantitative and real-time version of colorimetric LAMP. Fig. 4C shows the results from a series of experiments in which we followed the evolution of the LAMP reaction, in real time, in samples containing different quantities of synthetic genetic material (*i.e.*; 10 000, 1000, and 100 copies). We used an in-house set-up, based on the use of a commercially available and low cost (~40 USD) color sensor (EZO-RGB™, from Atlas Scientific) and an Arduino-based system to conduct these proof-of-concept real-time determinations. This sensor reports the R (red), G (green), and B (blue) components of color in the RGB color space and the *a*, *b*, *Y* components of the CIELAb color space, where *a* varies from 0 to 50, *b* varies from 0 to 50, and *Y* (the luminosity) varies from 0 to 100. We continuously calculated the distance in color in the $a \times b$ plane during amplification experiments. The initial coordinates of color of the sample were taken as a point of reference to calculate the distance in color. We observed trends that are consistent with the data obtained from discrete timepoints (Fig. 3). The color of the reaction mix changes progressively as the incubation time advances. The evolution of the color distance in the CIELab space shows similar trends in samples containing 100, 1000, and 10 000 synthetic viral copies. That is, the shape of the amplification curve is similar in all positive cases. The color of negative samples also evolves in time; however, the extent and slope of the color change are significantly lower than those observed in positive cases. The distance between the original color and the final color is greater than 1.5 units in all positive cases and smaller than 0.75 distance units in negative samples.

Moreover, the point at which each curve starts rising is consistent (and correlated) with the copy number (Fig. 4D). As expected, the curve corresponding to 10 000 copies rises sooner than the curve corresponding to 1000 copies, followed by the curve corresponding to 100 copies. We calculated the initial point of time at which the color distance consistently surpasses one standard deviation of the baseline signal. On average, these time values are 8.66 ± 0.50, 14.122 ± 0.91, and 21.08 ± 1.05 minutes for samples containing 10 000, 1000, and 100 synthetic copies of the N gene of SARS-CoV-2, respectively. Our experimental setup (ESI Fig. S4†) for continuous determination of color distances during LAMP reactions exhibits limitations for widespread implementation and is certainly amenable to optimization. However, it illustrates the feasibility and usefulness

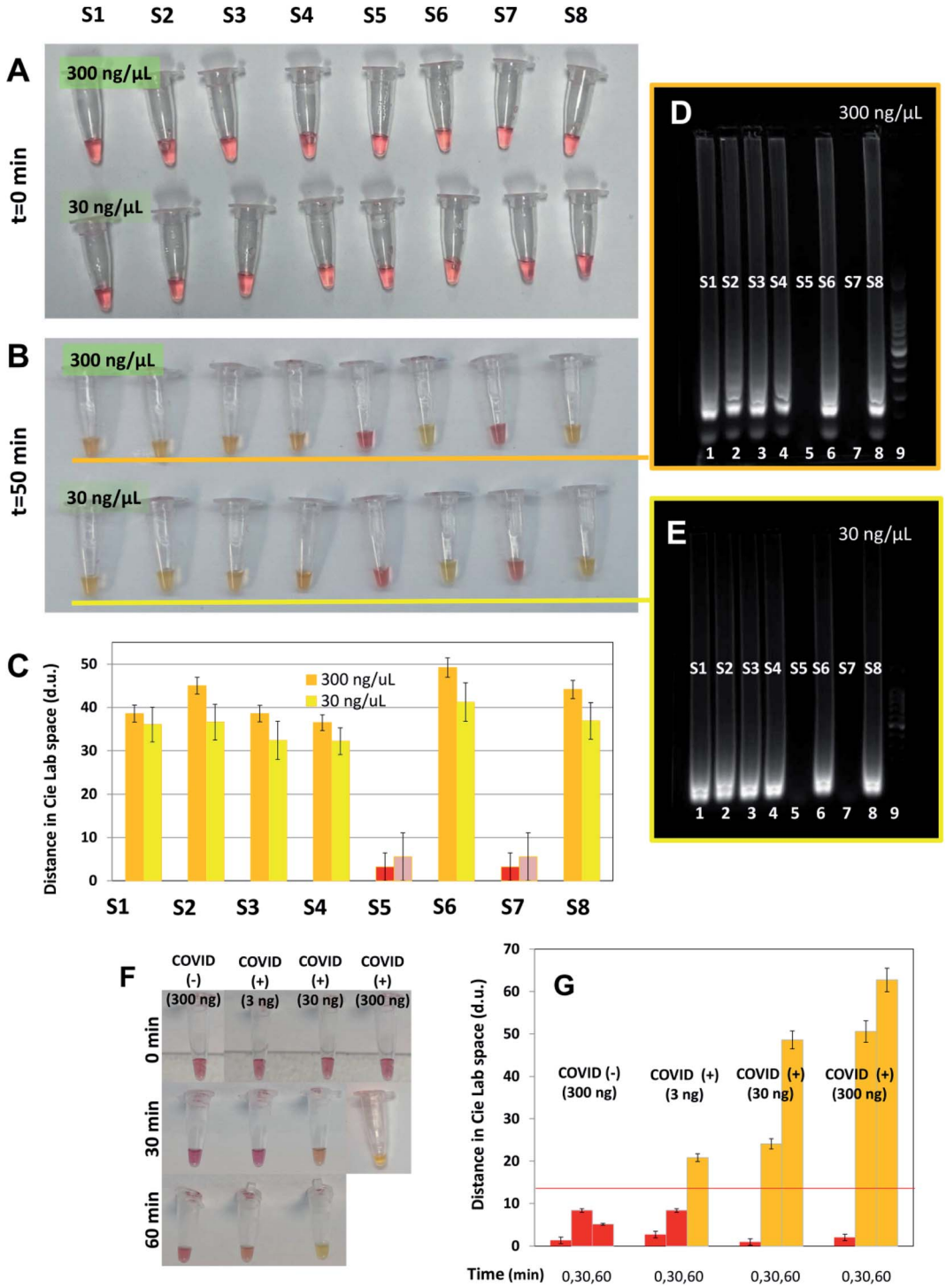

Fig. 5 Discrimination of actual RNA extracts from COVID-19 positive and negative samples. Color of RNA extracts from 6 COVID-19(+) and 2 COVID-19(−) samples, at two different concentrations (300 and 30 ng μL^{-1}), (A) before, and (B) after colorimetric LAMP reaction. COVID-19 positive samples (S1, S2, S3, S4, S6, and S8) can be easily discriminated by visual inspection. (C) Distance in color of samples of RNA extracts with respect to negative samples (S5 and S7) in the CIELab space. Distances in color of samples containing 300 ng of nucleic acids (orange bars), or 30 ng of nucleic acids (yellow bars) are presented. (D and E) LAMP amplification products from RNA extracts containing (D) 300 ng μL^{-1} and (E) 30 ng μL^{-1} from the same set of COVID(+) patients (S1–S4, S6 and S8), and COVID(−) volunteers (S5 and S7), as revealed by gel electrophoresis experiments. Lanes 1 to 8 contained amplification products from samples S1 to S8. Lane 9 was reserved for the molecular weight ladder (Fig. S6†). (F) Time progression of color changes in LAMP reaction mixes containing 300 ng of RNA extract from a COVID(−) volunteer (as diagnosed by RT-qPCR), and 3, 30, and 300 ng of RNA extract from a COVID(+) patient (as diagnosed by RT-qPCR). (G) Distance in color with respect to negative controls (red color) in the CIELab space for RNA extracts from a COVID(−) volunteer (as diagnosed by RT-qPCR) containing 300 ng of nucleic acids, and a COVID(+) patient (as diagnosed by RT-qPCR) containing 3, 30, and 300 ng of nucleic acids. Readings at 0, 30, and 60 minutes are shown. A suggested positive–negative threshold value is indicated with a red line.

of real-time color sensing for conferring a quantitative character to colorimetric LAMP.

Alternatively, the progression of the amplification at different times was monitored by adding an intercalating DNA agent (*i.e.*, EvaGreen Dye), and measuring fluorescence on time (Fig. S5†). Note that the variance coefficients for the control are 1.08, 7.50, and 8.10% for L, a, and b, respectively. These small values suggest robustness and reproducibility in the location of the coordinates of the control point (reference point). Similarly, the variation in color between negative controls and positive samples incubated for 50 min was reproducible and robust (average of 46.60 ± 4.02 d.u.; variance coefficient of 8.62%).

We observed an exponential increase in fluorescence as more LAMP or PCR cycles were performed, which highlights the quantitative nature of the intercalating reaction. The LAMP reaction produces significantly higher fluorescence signals that the PCR reaction throughout the entire reaction time. The difference between the fluorescence emissions of both amplifications is more evident after the first 20 minutes of amplification. These results also suggest that using a commercial plate reader to determine the extent of advance of LAMP amplifications is a practical and reliable alternative to the use of colorimetric evaluations. Moreover, fluorescence reading of LAMP products may lead to precise quantification of SARS-CoV-2 viral loads. In an additional set of experiments, synthetic samples that contained nucleic acids of SARS-CoV-2 equivalent to 1×10^4 viral copies were amplified by PCR and LAMP. During amplification, the products were marked with intercalating reagent. At different time points throughout amplification, the samples was dispensed in 96-week plates, and their fluorescence was then measured in a commercial plate reader[23] (Fig. 4E).

We also compared the performance of RT-qPCR and colorimetric LAMP using actual RNA extracts isolated from human volunteers. In a first experiment, we blind tested a set of 2 extracts of human RNA from nasopharyngeal samples of patients that were diagnosed as COVID-19(−) and 6 samples from patients diagnosed as COVID-19(+) by RT-qPCR (Fig. 5). We adjust the RNA content in all samples to 300 ng μL^{-1} of RNA. Then, samples were serially diluted (to 30 and 3 ng μL^{-1}) to challenge the sensitivity of colorimetric LAMP. All samples, undiluted and diluted, were added with the LAMP reactive mix and incubated at 65 °C by 50 minutes. All samples exhibit a red color before incubation (Fig. 5A), and only positive samples shifted to yellow during incubation (Fig. 5B). We were able to discriminate between positive and negative samples in the entire concentration range tested (300, 30, and 3 ng of total RNA, as determined by nanoDrop assays). The color shift (red to yellow) was clearly perceived after 30 minutes of amplification in samples containing 300 ng of total RNA from COVID(+) patients, 50 minutes in samples containing 30 and 3 ng of total RNA. COVID-19 positive RNA samples, original or diluted, showed similar values of distance in color with respect to negative samples, although standard deviations were higher in samples that contained 30 ng μL^{-1} than in samples that contained 300 ng μL^{-1} (Fig. 5C). We confirmed results by gel electrophoresis of the amplification products. Only positive samples exhibited the characteristic DNA profile associated with LAMP products (Fig. 5D and E).

In this reduced but representative set of extracts from nasopharyngeal patient samples, diagnostic results from colorimetric LAMP were completely consistent with RT-qPCR results, and similar results were obtained regardless of the LAMP primer set used (*i.e.*, α and β). Moreover, discrimination of positive samples even in diluted samples suggests that this colorimetric technique may be useful even in situations where the amount of RNA extracted is low due to improper sampling/extraction or degradation during transportation (Fig. 5F and G). Our experiments show that the distance in color between positive and negative RNA samples from human volunteers is proportional to the number of viral copies. These results suggest that the change in color can be quantitatively related to the viral load of SARS-CoV-2 in actual RNA extracts, similarly to synthetic samples. In an extension of this experiment, we included additional samples from RNA extracts of patients diagnosed by RT-qPCR at a local hospital (Medical Alfa, S.A. de C.V.). For this extended pool, LAMP reaction was restricted to 30 minutes of incubation. Overall, 28 extracts from COVID-19(+) patients and 16 COVID-19(−) patients, as diagnosed by RT-PCR, were analyzed. From these 28 extracts from COVID-19 patients, our LAMP-based method saw 26/28 as positive for a sensitivity of 92.85%. From the 16 samples of COVID-19(−) patients that we have analyzed, our LAMP-based method identified 13/16 as negative. This yields a specificity of 81.25%.

Validation of our results using a larger number of real human samples is needed to obtain a full assessment of the potential of this strategy as an alternative to RT-qPCR platforms. However, our results with synthetic samples and with a reduced number of samples containing RNA from human volunteers ($n = 42$) suggest that this simple strategy may greatly enhance the capabilities for COVID-19 testing.

Conclusions

Here, we have demonstrated that a simple embodiment of a LAMP reaction, assisted by the use of phenol red as a pH indicator, can enable the rapid and highly accurate identification of samples that contain artificial SARS-CoV-2 genetic sequences. We also showed, using synthetic SARS-CoV-2 and a reduced number of RNA extracts from patients ($n = 42$), that colorimetric LAMP is a quantitative method, comparable to RT-qPCR. Amplification is visually evident, without the need for any additional instrumentation, even at low viral copy numbers. In our experiments with synthetic samples, we observed 100% accuracy in samples containing as few as 62.5 copies of SARS-CoV-2 genetic material. We observed a sensitivity of 92.85% and specificity of 81.25% when this embodiment of colorimetric LAMP was conducted on RNA extracts from patients in a hospital environment.

In the current context of the COVID-19 pandemics, the method described here competes with other molecular methods in accuracy, and surpasses RT-qPCR is cost-effectiveness. While the market value of a traditional RT-qPCR apparatus (the current gold standard for COVID-19

diagnostics) is in the range of 10 000 to 40 000 USD, a miniPCR and a thermo-block may cost ~800 and 250 USD, respectively. These differences in capital investment between RT-qPCR and colorimetric LAMP are significant, especially during an epidemic or pandemic crisis when rational investment of resources is critical. While the quantitative capabilities of testing using an RT-qPCR platform are undisputable, the capacity of many countries to rapidly, effectively, and massively establish diagnostic centers based on RT-qPCR is questionable. The current pandemic scenarios experienced in the USA, England, Italy, France, and Spain, among others, have crudely demonstrated that centralized labs are not an ideal solution during emergencies. The situation in highly populated developing countries such as Brazil, México or India is even worst. Portable diagnostic systems may provide a vital flexibility and speed of response that RT-qPCR platforms cannot deliver.

Materials and methods

Equipment specifications

We ran amplification experiments using a colorimetric LAMP method in a miniPCR mini8 thermal cycler (Amplyus, MA, USA) operated isothermally at 60 or 65 °C. We used an electrophoresis unit, powered by 120 AC volts, to validate the LAMP amplification using gel electrophoresis. Photo-documentation of color in LAMP samples was done using a smartphone camera. We also used a Synergy HT microplate reader (BioTek Instruments, VT, USA) to detect the fluorescence induced by an intercalating reagent in positive samples from the LAMP and PCR reactions.

Validation DNA templates

We used plasmids containing the complete N gene from SARS-CoV-2 as a positive control (Fig. S7†), with a concentration of 200 000 copies per μL (Integrated DNA Technologies, IA, USA). Samples containing different concentrations of synthetic nucleic acids of SARS-CoV-2 were prepared by successive dilutions from stocks (from 2×10^5 copies to 65 copies).

RNA extracts from human volunteers

In addition, we used samples of RNA extracts from 28 COVID-19 positive and 14 negative subjects, as determined by RT-PCR analysis. Samples were kindly donated by Hospital Alfa, Medical Center, in Guadalupe, Nuevo León, México. Nasopharyngeal samples were collected from patients after obtaining informed and signed written consent and in full compliance with good clinical practices, the principles stated in the Helsinki Declaration, and applicable lab operating procedures at Hospital Alfa. Every precaution was taken to protect the privacy of sample donors and the confidentiality of their personal information. The experimental protocol was approved on May 20th, 2020 by a named institutional committee (Alfa Medical Center, Research Committee; resolution AMCCI-TECCOVID-001).

Amplification mix

We used WarmStart® Colorimetric LAMP 2× Master Mix (DNA & RNA) from New England Biolabs (MA, USA), and followed the recommended protocol: 12.5 μL Readymix, 1.6 μM FIP primer, 1.6 μM BIP primer, 0.2 μM F3 primer, 0.2 μM B3 primer, 0.4 μM LF primer, 0.4 μM LB primer, 1 μL DNA template (~ 625 to 2 × 105 DNA copies), 1.25 μL EvaGreen® Dye from Biotium (CA, USA), and nuclease-free water to a final volume of reaction 25 μL. This commercial mix contains phenol red as a pH indicator for revealing the shift of pH during LAMP amplification across the threshold of pH = 6.8.

Primers used

Two different sets of LAMP primers, referred here as α and β, were designed in house using the LAMP primer design software Primer Explorer V5 (http://primerexplorer.jp/lampv5e/index.html).

These primers were based on the analysis of alignments of the SARS-CoV-2 N gene sequences using the software Geneious (Auckland, New Zealand), downloaded from https://www.ncbi.nlm.nih.gov/genbank/sars-cov-2-seqs/#nucleotide-sequences.

Each set, containing six LAMP primers, were used to target two different regions of the sequence of the SARS-CoV-2 N gene. In addition, for comparison purposes, we conducted PCR amplification experiments using one of the primer sets recommended by the CDC for the standard diagnostics of COVID-19 (*i.e.*, N1 assay) using RT-qPCR. The sequences of our LAMP primers are presented in Table 1. The sequences of the PCR primers (N1) have been reported elsewhere.[23,49]

Amplification protocols

For all LAMP experiments, we performed isothermal heating for 30 or 60 min. In our experiments, we tested three different temperatures: 50, 60, and 65 °C.

For PCR experiments, we used a three-stage protocol consisting of a denaturation stage at 94 °C for 5 min, followed by 25 cycles of 94 °C for 20 s, 60 °C for 30 s, and 72 °C for 20 s, and then a final stage at 72 °C for 5 min, for a total duration of 60 min in the miniPCR® thermocycler from Amplyus (MA, USA).

Documentation of LAMP products

We analyzed 10 μL of each LAMP reaction in a blueGel unit, a portable electrophoresis unit sold by MiniPCR from Amplyus (MA, USA). In these experiments, we analyzed 10 μL of the LAMP product using 1.2% agarose electrophoresis tris-borate-EDTA buffer (TBE). We used the Quick-Load Purple 2-Log DNA Ladder (NEB, MA, USA) as a molecular weight marker. Gels were dyed with Gel-Green from Biotium (CA, USA) using a 1 : 10 000 dilution, and a current of 48 V was supplied by the blueGel built-in power supply (AC 100–240 V, 50–60 Hz).

As an alternative method for detection and reading of the amplification product, we evaluated the amplification products by detecting the fluorescence emitted by a DNA-intercalating

agent, the EvaGreen® Dye from Biotium (CA, USA), in a Synergy HT microplate reader (BioTek Instruments, VT, USA). Briefly, 25 μL of the LAMP reaction was placed in separate wells of a 96-well plate following completion of the LAMP incubation. A 125 μL volume of nuclease-free water was added to each well for a final sample volume of 150 μL and the samples were well-mixed by pipetting. These experiments were run in triplicate. The following conditions were used in the microplate reader: excitation of 485/20, emission of 528/20, gain of 75. Fluorescence readings were done from the top at room temperature.

Color determination by image analysis

We photographically documented and analyzed the progression of color changes in the positive and negative SARS-CoV-2 synthetic samples during the LAMP reaction time (*i.e.*, from 0 to 50 min). For that purpose, Eppendorf PCR tubes containing LAMP samples were photographed using a smartphone (iPhone, from Apple, USA). We used an application for IOS (Color Companion, freely available at Apple store) to determine the components of color of each LAMP sample in the CIELab color space. Color differences between the positive samples and negative controls were calculated as distances in the CIELab coordinate system according to the following formula:

$$\text{Color distance}_{\text{sample-negative}} = \text{SQRT}[(L_{\text{sample}} - L_{\text{negative}})^2 + (a_{\text{sample}} - a_{\text{negative}})^2 + (b_{\text{sample}} - b_{\text{negative}})^2]$$

Here L, a, and b are the color components of the sample or the negative control in the CIELab color space (Fig. S3†).

On-line color determination

We also monitored the color progression of samples containing SARS-CoV-2 synthetic material during LAMP reactions using an on-line EZO-RGB color sensor (Atlas Scientific, USA). The sensor was controlled by an Arduino-Uno microprocessor. The sensor was placed over the flat monitor of a laptop that received a real-time video of the Eppendorf tube incubated at 62 °C in a water bath. Video was obtained using a USB camera (SVPRO USB 5–50 mm varifocal lens, 8 megapixel, 3264 × 2448 Industrial USB camera; from SVPRO; bought at http://Amazon.com). The Zoom™ platform (USA) was used for video capture and recording. A Spectre™ HP laptop (USA) was used for simultaneous video recording and on-line data collection from the Arduino-based sensing system. A Puluz™ photo light box (upgraded version 30 cm, from Puluz; available at Mercado Libre, México) was used to provide a controlled and constant illumination environment.

Author participation

E. G. and I. L. conducted most of the LAMP amplification experiments; M. A. and G. T. designed and built the on-line colorimetric LAMP system and conducted the real-time LAMP experiments; I. R. performed all RNA extractions from nasal samples and RT-qPCR experiments at Alfa Medical; G. T. and M. A. wrote the manuscript; E. G. I. L. and M. A. prepared the figures; Y.-S. Z., S. M., M. A. and G. T., edited the manuscript; and G. T., S. M., E. G., and M. A. designed the study.

Conflicts of interest

E. G., I. L., M. A., and G. T. have submitted a PCT patent application on primer sets α and β. E. G., M. A., and G. T. currently sustain technical collaboration with AimBrands Co. (Bentonville, AR; USA).

Acknowledgements

The authors acknowledge the funding provided by the Federico Baur Endowed Chair in Nanotechnology (0020240I03). M. A., G. T., S. M., I. R., and I. L. acknowledge funding provided by CONACyT (Consejo Nacional de Ciencia y Tecnología, México) through SNI (Sistema Nacional de Investigadores) scholarships. E.G. acknowledges funding from a doctoral scholarship provided by CONACyT (Consejo Nacional de Ciencia y Tecnología, México). G. T. and M. A. acknowledge the institutional funding received from Tecnológico de Monterrey (Grant 002EICI04). Y.-S. Z. acknowledges the support by the Brigham Research Institute. We are grateful to Felipe Yee-de León, Andrés García-Rubio, Carlos Ezio Garcíamendez-Mijares, Gilberto Emilio Guerra-Alvarez, Germán García-Martínez, Juán Andrés Aguayo-Hernández, Sergio Bravo-González, and Eduardo Márquez-García for their experimental support.

Notes and references

1 *Coronavirus Disease (COVID-19) – Statistics and Research – Our World in Data*, https://ourworldindata.org/coronavirus?fbclid=IwAR28tcRVA1rmXsVCrYHcxuHpRXeyO9-uxFJFSG5-lv5gsJgzDxK7eN08i_Y, accessed 8 April 2020.
2 J. Bedford, D. Enria, J. Giesecke, D. L. Heymann, C. Ihekweazu, G. Kobinger, H. C. Lane, Z. Memish, M. don Oh, A. A. Sall, A. Schuchat, K. Ungchusak and L. H. Wieler, *Lancet*, 2020, **395**, 1015–1018.
3 J. Cohen and K. Kupferschmidt, *Science*, 2020, **367**, 1287–1288.
4 R. Pung, C. J. Chiew, B. E. Young, S. Chin, M. I.-C. Chen, H. E. Clapham, A. R. Cook, S. Maurer-Stroh, M. P. H. S. Toh, C. Poh, M. Low, J. Lum, V. T. J Koh, T. M. Mak, L. Cui, R. V. T. P. Lin, D. Heng, Y.-S. Leo, D. C. Lye and V. J. M Lee, *Lancet*, 2020, **19**, 1–8.
5 M. M. Alvarez, E. Gonzalez-Gonzalez and G. T. Santiago, *medRxiv*, 2020, DOI: 10.1101/2020.03.23.20041590.
6 P. Abraham, N. Aggarwal, G. R. Babu, S. Barani, B. Bhargava, T. Bhatnagar, A. S. Dhama, R. R. Gangakhedkar, S. Giri, N. Gupta, K. K. Kurup, M. Murhekar, V. Potdar, I. Praharaj, K. Rade, D. C. S. Reddy, V. Saravanakumar, N. Shah, H. Singh, J. W. V. Thangaraj and N. Yadav, *Indian J. Med. Res.*, 2020, **151**, 424–437.
7 F. A. L. Marson, *Diagn. Microbiol. Infect. Dis.*, 2020, **98**, 115113.
8 C.-W. Yen, H. de Puig, J. O. Tam, J. Gómez-Márquez, I. Bosch, K. Hamad-Schifferli and L. Gehrke, *Lab Chip*, 2015, **15**, 1638–1641.

9 L. Mou and X. Jiang, *Adv. Healthcare Mater.*, 2017, **6**, 1601403.
10 M. M. Alvarez, F. López-Pacheco, J. M. Aguilar-Yañez, R. Portillo-Lara, G. I. Mendoza-Ochoa, S. García-Echauri, P. Freiden, S. Schultz-Cherry, M. I. Zertuche-Guerra, D. Bulnes-Abundis, J. Salgado-Gallegos, L. Elizondo-Montemayor and M. Hernández-Torre, *PLoS One*, 2010, **5**, e10176.
11 L. Zhong, J. Chuan, B. Gong, P. Shuai, Y. Zhou, Y. Zhang, Z. Jiang, D. Zhang, X. Liu, S. Ma, Y. Huang, H. Lin, Q. Wang, L. Huang, D. Jiang, F. Hao, J. Tang, C. Zheng, H. Yu, Z. Wang, Q. Jiang, T. Zeng, M. Luo, F. Zeng, F. Zeng, J. Liu, J. Tian, Y. Xu, T. Long, K. Xu, X. Yang, Y. Liu, Y. Shi, L. Jiang and Z. Yang, *Sci. China: Life Sci.*, 2020, **63**, 777–780.
12 K. Pardee, A. A. Green, M. K. Takahashi, D. Braff, G. Lambert, J. W. Lee, T. Ferrante, D. Ma, N. Donghia, M. Fan, N. M. Daringer, I. Bosch, D. M. Dudley, D. H. O'Connor, L. Gehrke and J. J. Collins, *Cell*, 2016, **165**, 1255–1266.
13 Z. Huang, D. Tian, Y. Liu, Z. Lin, C. J. Lyon, W. Lai, D. Fusco, A. Drouin, X. Yin, T. Hu and B. Ning, *Biosens. Bioelectron.*, 2020, **164**, 112316.
14 L. Elizondo-Montemayor, M. M. Alvarez, M. Hernández-Torre, P. A. Ugalde-Casas, L. Lam-Franco, H. Bustamante-Careaga, F. Castilleja-Leal, J. Contreras-Castillo, H. Moreno-Sánchez, D. Tamargo-Barrera, F. López-Pacheco, P. J. Freiden and S. Schultz-Cherry, *Int. J. Infect. Dis.*, 2011, **15**, e781–e786.
15 Y.-W. Tang, J. E. Schmitz, D. H. Persing and C. W. Stratton, *J. Clin. Microbiol.*, 2020, **58**(6), e00512-20.
16 R. Wölfel, V. M. Corman, W. Guggemos, M. Seilmaier, S. Zange, M. A. Müller, D. Niemeyer, T. C. Jones, P. Vollmar, C. Rothe, M. Hoelscher, T. Bleicker, S. Brünink, J. Schneider, R. Ehmann, K. Zwirglmaier, C. Drosten and C. Wendtner, *Nature*, 2020, 1–10.
17 M. G. Mauk, J. Song, H. H. Bau and C. Liu, *Clinical laboratory International*, 2017, **41**, 25–27.
18 S.-C. Liao, J. Peng, M. G. Mauk, S. Awasthi, J. Song, H. Friedman, H. H. Bau and C. Liu, *Sens. Actuators, B*, 2016, **229**, 232–238.
19 P. Jansen van Vuren, A. Grobbelaar, N. Storm, O. Conteh, K. Konneh, A. Kamara, I. Sanne and J. T. Paweska, *J. Clin. Microbiol.*, 2016, **54**, 359–367.
20 P. Craw and W. Balachandran, *Lab Chip*, 2012, **12**, 2469.
21 K. Hsieh, A. S. Patterson, B. S. Ferguson, K. W. Plaxco and H. T. Soh, *Angew. Chem., Int. Ed. Engl.*, 2012, **51**, 4896–4900.
22 E. González-González, J. L. Mendoza-Ramos, S. C. Pedroza, A. A. Cuellar-Monterrubio, A. R. Márquez-Ipiña, D. Lira-Serhan, G. Trujillo-de Santiago and M. M. Alvarez, *PLoS One*, 2019, **14**, e0215642.
23 E. Gonzalez-Gonzalez, G. Trujillo-de Santiago, I. M. Lara-Mayorga, S. O. Martinez-Chapa and M. M. Alvarez, *PLoS ONE*, 2020, **15**, e0237418.
24 R. Lei, X. Wang, D. Zhang, Y. Liu, Q. Chen and N. Jiang, *Sci. Rep.*, 2020, **10**, 1–11.
25 K. Kaarj, P. Akarapipad and J. Y. Yoon, *Sci. Rep.*, 2018, **8**, 1–11.
26 N. Tomita, Y. Mori, H. Kanda and T. Notomi, *Nat. Protoc.*, 2008, **3**, 877–882.
27 M. Goto, E. Honda, A. Ogura, A. Nomoto and K. I. Hanaki, *Biotechniques*, 2009, **46**, 167–172.
28 T. Yang, Y.-C. Wang, C.-F. Shen and C.-M. Cheng, *Diagnostics*, 2020, **10**, 165.
29 T. R. Kozel and A. R. Burnham-Marusich, *J. Clin. Microbiol.*, 2017, **55**, 2313–2320.
30 W. Su, X. Gao, L. Jiang and J. Qin, *J. Chromatogr. A*, 2015, **1377**, 13–26.
31 M. Drancourt, A. Michel-Lepage, S. Boyer and D. Raoult, *Clin. Microbiol. Rev.*, 2016, **29**, 429–447.
32 S. R. Jangam, A. K. Agarwal, K. Sur and D. M. Kelso, *Biosens. Bioelectron.*, 2013, **42**, 69–75.
33 X. Qiu, S. Ge, P. Gao, K. Li, S. Yang, S. Zhang, X. Ye, N. Xia and S. Qian, *Microsyst. Technol.*, 2017, **23**, 2951–2956.
34 T. Nguyen, D. Duong Bang and A. Wolff, *Micromachines*, 2020, **11**, 306.
35 B. Udugama, P. Kadhiresan, H. N. Kozlowski, A. Malekjahani, M. Osborne, V. Y. C. Li, H. Chen, S. Mubareka, J. Gubbay and W. C. W. Chan, *ACS Nano*, 2020, **14**, 3822–3835.
36 B. Gates, *N. Engl. J. Med.*, 2020, **382**, 1677–1679.
37 Y. Zhang, N. Odiwuor, J. Xiong, L. Sun, R. O. Nyaruaba, H. Wei and N. A. Tanner, *medRxiv*, 2020, **2**, DOI: 10.1101/2020.02.26.20028373.
38 D. Wang, B. Hu, C. Hu, F. Zhu, X. Liu, J. Zhang, B. Wang, H. Xiang, Z. Cheng, Y. Xiong, Y. Zhao, Y. Li, X. Wang and Z. Peng, *JAMA, J. Am. Med. Assoc.*, 2020, **323**, 1061–1069.
39 X. Zhu, X. Wang, L. Han, T. Chen, L. Wang, H. Li, S. Li, L. He, X. Fu, S. Chen, X. Mei, H. Chen and Y. Wang, *Biosens. Bioelectron.*, 2020, **166**, 112437.
40 L. E. Lamb, S. N. Bartolone, E. Ward and M. B. Chancellor, *PLoS One*, 2020, **15**, e0234682.
41 M. Jiang, W. Pan, A. Arasthfer, W. Fang, L. Ling, H. Fang, F. Daneshnia, J. Yu, W. Liao, H. Pei, X. Li and C. Lass-Flörl, *Front. Cell. Infect. Microbiol.*, 2020, **10**, 331.
42 L. Yu, S. Wu, X. Hao, X. Dong, L. Mao, V. Pelechano, W. H. Chen and X. Yin, *Clin. Chem.*, 2020, **66**, 975–977.
43 V. L. D. Thi, K. Herbst, K. Boerner, M. Meurer, L. P. Kremer, D. Kirrmaier, A. Freistaedter, D. Papagiannidis, C. Galmozzi, M. L. Stanifer, S. Boulant, S. Klein, P. Chlanda, D. Khalid, I. Barreto Miranda, P. Schnitzler, H.-G. Kräusslich, M. Knop and S. Anders, *Sci. Transl. Med.*, 2020, **12**, eabc7075.
44 G. Trujillo-de Santiago, C. Rojas-De Gante, S. García-Lara, A. Ballescá-Estrada and M. M. Alvarez, *PLoS One*, 2014, **9**, e112954.
45 N. A. Tanner, Y. Zhang and T. C. Evans, *Biotechniques*, 2015, **58**, 59–68.
46 N. Rusk, *Nat. Methods*, 2011, **8**, 44.
47 W. Wang, Y. Xu, R. Gao, R. Lu, K. Han, G. Wu and W. Tan, *JAMA, J. Am. Med. Assoc.*, 2020, **323**, 1843–1844.
48 L. Yu, S. Wu, X. Hao, X. Dong, L. Mao, V. Pelechano, W-H. Chen and X. Yin, *Clin. Chem.*, 2020, **66**, 975–977.
49 OSF preprints|landscape coronavirus disease 2019 test (COVID-19 test) in vitro – a comparison of PCR vs. immunoassay vs. Crispr-based test, https://osf.io/6eagn, accessed 8 April 2020.

